THE MIT HIGH DUTY, HIGH INTENSITY 400 MEV LINEAR ELECTRON ACCELERATOR

W. Bertozzi, J. Haimson, C.P. Sargent, W. Turchinetz

Laboratory for Nuclear Science
Massachusetts Institute of Technology
Cambridge, Massachusetts

A 400 MeV high duty ratio, high intensity linear electron accelerator is under design by the Laboratory for Nuclear Science of MIT under the sponsorship of the AEC. This paper reports design objectives and describes component systems, including the buildings, RF power transmitters, beam centerline, beam transport system, and some experimental equipment planned for the facility.

Introduction

It has become clear in recent years, largely as a result of work done at Stanford and Orsay, that research with electron beams of fairly high energy, 1 GeV or so, will continue to be a source of important information on nuclear structure. Since the cross-sections one wishes to investigate are small, beams of high intensity and good energy homogeneity are required. High intensity is also important to realize useful secondary beams of pions, neutrons, positrons, and photons. For much of this research it is necessary to observe a scattered electron in coincidence with one or more reaction products in order to specify adequately the reaction kinematics. To reduce accidental coincidences in this type of experiment, the duty ratio must be much higher than that available at Stanford and Orsay, and should be at least comparable with the duty normally obtained with electron synchrotrons. It is to meet the need for this type of high intensity, high duty intermediate energy accelerator that the MIT linac and the similar accelerator at Saclay (A.L.S.) are being built.

The MIT linac will consist of approximately 530 feet of constant gradient S band waveguide, powered by ten klystrons rated at 4 MW, 80 KW each. With a maximum design energy of 440 MeV, this implies a maximum accelerating gradient less than one MeV per foot. This low electric field gradient, imposed by the high duty ratio requirement for low RF peak power, together with the narrow energy spectra design objective of 50% current through 0.4% energy analyzing slits, has given rise to several new design approaches. Important among these are: The use of high voltage direct switching series type modulators; the injection of RF chopped monochromatic bunches of narrow phase width into a low gradient variable phase velocity traveling wave buncher; and the use of long accelerator waveguides designed to operate over a wide range of duty cycle and beam loading.

Accelerator Beam Specifications

The following specifications refer to accelerator design objectives. When two numbers are given separated by a hyphen, the first number refers to 1 MW peak power operation of the klystrons and the second to 4 MW operation.

Electron beam energy (unloaded)	220-440 MeV
Electron beam energy(10% loading	198-396 MeV
Peak beam current (10% loading)	7-16 mA.
Beam duty cycle, maximum	5.8-1.8 %
Average beam current(10% loading)	405-288 μA.
Beam pulse length, maximum	15 μsec.
Pulse repetition rate, maximum	5000 pps.
Phase width of electron bunch, maximum	5°
Radial phase space	$4 \times 10^{-3} \pi$ mc-cm
Energy spread for 50% current	$\pm$ 0.2%

Buildings and Site

Architectural and engineering studies for the facility are now in progress. The schedule calls for the start of construction before September 1967, with occupancy by the end of 1968 and beam tests to be underway by the summer of 1969. The 80 acre site is located in Middleton, Mass., on a glacial drumlin. The dense till provides an exceptionally stable bearing support for the accelerator.

A vault, ten feet square by 600 feet long, will contain the beam centerline structure. It will begin at a station housing and servicing the injector, and will be followed by a beam switchyard complex leading to two experimental areas. The vault will be separated by 15 ft of earth from a 25 ft. wide gallery containing the RF power equipment. Paralleling the switchyard area will be about 9000 sq. ft. of control and laboratory space. One of the experimental areas contains about 1500 sq. ft., and the second about 3000 sq. feet. This latter is designed to house a pair of high resolution spectrometers (see Experimental Equipment).

Transmitters

Figure 1 shows the arrangement of the centerline waveguide, klystrons, modulators, and power supplies. The waveguide complement will include: 1) a 10 MeV injector for which one klystron is reserved, 2) four 12 ft. sections powered by a second klystron, and 3) twenty long 24 ft. sections. The long sections will be connected, as shown, so that six klystrons service twelve sections, and two klystrons the last eight sections.

Each klystron will operate over an output power range extending from 1 MW peak, 65 KW average to 4 MW peak, 80 KW average with about 100 watts peak drive power per klystron. Collector dissipation capability will be 300 KW, with RF pulse lenghts to 16 microseconds. There will be a single output window per klystron, the output passing from the klystron through a short section of pressurized waveguide before entering the evacuated guide system leading to the accelerating structure.

Modulator specifications call for not more than 0.15% beam voltage modulation peak to peak over the 15 μsec flat-top region at all output powers in the 1 to 4 megawatt range. The voltage jitter limitation, over one second, is also 0.15% and the drift, over one hour, 0.25%.

The transmitters will represent a new approach to high power pulse modulators, one that has been chosen over alternate schemes both on the basis of economy and also as being the method most likely to achieve reliably the very high quality specifications. Two other techniques were judged capable of at least approaching the specifications, and were given serious consideration. The first involves the use of a mod anode klystron and a switch-deck type modulator, and was ruled out principally on the basis of cost. The cost differential lies for the most part in the klystrons themselves and in their development, and in the rather complex methods of regulation required to obtain the necessary pulse-to-pulse stability. The second, more comparable in cost to the selected technique, involves a 30-40 kv hard tube modulator pulse transformer coupled to the klystron, similar to the NBS and ALS modulators. This scheme was judged to be less likely to meet the specifications, to be less efficient, and to possess less operational flexibility than the chosen scheme, although these minuses had to be weighed against the plus of the experience accumulated at NBS and in France.

The critical modulator component is the L-5097 switch tube. It will be a magnetron injection gun tube, a member of a family of tubes which have been used for several years as deck switches in mod anode klystron radar applications. It will be nearly identical to the most recent member of that family, the L-5033. However, in our system certain characteristics are required which have not been of importance in previous applications. These are very high plate resistance, low noise, and high dissipation capability at constant plate voltage. Recent tests indicate that the L-5033 meets the program requirements, although, as the L-5097, it will be modified slightly to enhance its power dissipation performance and improve the noise characteristics.

The tubes will be processed to 230 kv. The gridless construction is very rugged, with the cathode well protected from arcs. The high plate resistance is an essential characteristic, since it provides the regulation necessary for meeting the jitter and drift specifications, provides protection against the effects of power line transients, and allows economy in the energy storage capacitor banks. The plate resistance of the two switch tubes in parallel required per klystron will be more than ten times the dynamic resistance of the klystron.

Typical operation at the 4 MW RF output level with a 38% efficient klystron yields the following voltage budget: 122 kv (at 84.5 amps) across the klystron, 27 kv across the switch tubes (including an 8 kv allowance for a possible 5% negative going line transient), 1.5 kv capacitor bank droop (1 microfarad per klystron), and a 4 kv allowance for series resistor drop and power supply regulation, or a total supply voltage requirement of 154.5 kv. Rise time from 10% to 99% voltage should be about 1.7 μsec. Switch tube dissipation, including rise time effects, is about 32 kw per tube under the above normal full power operating conditions, although tubes will be rated at 60 kw, allowing full operational flexibility during tune-up.

Injector and Accelerator Waveguides

Figure 1 has indicated the centerline arrangement of injector, the four 12 ft.guides, and the twenty 24 ft. guides. An ABBA ABBA rectangular waveguide connection configuration has been adopted and RF couplers, symmetrized for longitudinal electric field intensity, will be used to minimize undesirable transverse momenta contributions to the beam.

The 10 MeV injector design consists essentially of a low perveance 100 KeV electron gun, a microwave chopper system, a traveling wave buncher, and a short high impedance accelerator waveguide section. The buncher is designed to avoid phase orbit cross-overs and to provide accelerating and bunching fields which approach the adiabatic condition.[1] The growth of space charge forces due to the shrinking bunch width is compensated by the increasing beam energy, taking care not to harden the beam too rapidly so that the bunching process may be continued over an extended length.

The attainment of very narrow ultimate bunch widths requires that special consideration be given to the problem of minimizing the variation of kinetic energy of the particles entering the traveling wave buncher. Even for the relatively low beam charge conditions being considered, because of the small dimensions of the chopped beam a twenty percent velocity modulation contribution would result from the action of space charge fields alone during flight through the drift tube. It is expected that the use of small diameter shielding circuits located within the drift tube and surrounding the beam can reduce velocity modulation content to the order of a few percent.

Each of the four short accelerator waveguides contain 104 $2\pi/3$ cavities which are arranged in a multiplicity of short uniform sections of increasing impedance, interconnected by transition regions. Allowing for rectangular waveguide losses, each section is designed for a zero beam loading energy gain of 10 MeV at an input RF peak power level of 0.85 MW. A fill time of 1.08 μsec has been chosen for these short sections.

The long waveguide sections consist of 210 2 $\pi/3$ cavities and are designed such that a constant gradient condition is approached at light beam loading. Each of the long sections that are connected two to a klystron have design zero beam loading energy gains of 22.5 MeV with 1.8 MW input RF peak power. The last eight accelerator sections, which are of the long design, will be connected four to a klystron, and for 0.85 MW input RF peak power each guide has a design energy gain of 15 MeV at zero beam loading.

The waveguide water cooling and vacuum requirements are particularly stringent owing to the various combinations and wide ranges of RF pulse length and repetition rate. A water flow of 100 GPM for each accelerator section has been specified to minimize the film and copper drops, and the overall temperature rise resulting from heat dissipation levels of up to 30 KW.

Figure 2 (a) shows typical copper loss distributions for one of the long waveguide designs and the following three operating conditions:

1.8 MW input RF peak power and zero beam loading - curve A,
1.8 MW input RF peak power and 25 mA beam loading - curve B, and
0.85 MW input RF peak power and zero beam loading - curve C.

Figure 2 (b) indicates that the increase in phase sensitivity towards the end of the section, due to the constant gradient requirement for reduced group velocity, occurs over a portion of the waveguide in which the copper losses are most affected by beam loading. (Compare curves A and B, Fig. 2 (a).) Thus in addition to bulk movement of the copper temperature distribution with change in duty factor, increased beam loading will result in a "chilling" effect which will be most pronounced over the more phase sensitive region of the structure.

Positioning of a metal temperature sensor at a specific location along the waveguide, best described as the temperature-phase distribution "fulcrum" point, can enable phase errors caused by a wide range of copper temperature distributions, to be corrected by automatic adjustment of the inlet water temperature. Waveguide copper temperature distributions and integrated phase error distributions based on an inlet water temperature of 45°C are shown as the "uncorrected" curves A, B and C in Fig. 2 (c) and (d), respectively, for the three heat dissipation examples of Fig. 2 (a) and a reference copper temperature of 45°C. The corresponding "corrected" distributions were computed with inlet water temperatures depressed by the same value as that required to maintain the copper reference temperature constant (45°C) at the location of the sensor. Steady-state corrections to within 2 or 3 degrees of total phase error appear realistic with this technique and are consistent with the intended 1/10°C temperature control and the long waveguide design value of 22 degrees of electrical phase shift per 1°C temperature rise. The above analysis refers to a uniflow water cooling system using twelve 0.43" ID tubes brazed directly onto the waveguide.

Beam Breakup Considerations

An extrapolation from SLAC data indicated that for the envisaged low field gradients, weak focusing, and long pulse length (15 μsec) conditions of operation, the multiple section[2,3] beam breakup phenomenon could impose a peak current limitation of the order of 5 mA. As a consequence, several alternate design approaches were investigated with the aim of elevating the threshold value associated with the HEM_{11} instability. This work established the progressive stop-band concept described below, and strongly influenced the deisgn of the accelerator waveguides. The technique is dependent upon maintaining a specific relationship along the beam center line between groups of waveguides of a particular design.

The twenty long waveguide sections comprise several groups each of which are similar in mechanical design but differ slightly in microwave characteristics. The HEM_{11} Brillouin characteristics of the first group of similar waveguides have been arranged such that the narrow band of closely spaced undesirable beam breakup frequencies, associated with the input coupler and uniform structures within the critical initial region of each waveguide, fall approximately 30 MHz outside and below the full range of HEM_{11} pass bands of all the subsequently located waveguides regardless of group affiliation. Correspondingly, the undesirable range of frequencies associated with the critical initial regions of the second group of waveguides has been designed to fall outside of the HEM_{11} pass bands associated with all of the remaining subsequently located waveguides. This procedure is maintained progressively along the full length of the accelerator. Physically, when using disc loaded waveguides of conventional construction, this technique requires that the initial disc iris dimensions of waveguides in a given group be smaller than those in all preceding groups but larger than those in all subsequently located groups.

The technique is illustrated diagrammatically in Fig. 3. Curves K,L,M and N represent typical TM_{11} Brillouin diagrams corresponding to uniform impedance 18 cavity structures having iris diameters of 30.48, 29.57, 28.45 and 26.42 mm, respectively. It can be noted that for each structure, and for the indicated range of iris dimensions, the undesirable resonances (phase slips per cavity $< \pi/10$) in the immediate vicinity of the $v_p = c$ intercept can be readily separated by slight adjustment of the iris diameter. In fact with separation sensitivity of this order (33 MHz/mm) the resonant stop-bands can be easily extended to regions of greater than 45° of slippage per cavity.

Impedance gaps (discontinuities) have also been designed into the structures in order to avoid HEM_{11} beam stimulation within the body of a waveguide at resonances corresponding to the undesirable (higher Q) initial regions of following accelerator sections i.e., the transition circuits neighbouring the unwanted uniform impedance zones are merged directly together. Application of this technique is somewhat restricted for waveguides of an earlier located group owing to the larger number of following groups. The disadvantage can be offset, however, by varying the number of cavities in the subject uniform impedance zones so that the phase slip dependent HEM_{11} frequency selection process is disturbed with respect to similar impedance sections in other waveguides. A programmed azimuthal variation of the deformation plane during tuning[4] of the accelerator waveguides is also planned.

In addition to these design approaches, aimed at reducing gross amplification effects along the accelerator by avoiding HEM_{11} spatial and temporal coherency, several local Q-spoiling techniques for higher order modes in the vicinity of the input coupler are currently being investigated.

Beam Transport System

The beam transport system extends over about 70 meters of underground vault from the end of the accelerator to the experimental areas. It provides three beams by means of four bending magnets, six quadrupole lenses, two slits, and an input collimator. The arrangement of these elements and characteristics of the beams are shown in Fig.4. A solenoid and a quadrupole Q7 are also indicated in this figure along Beam C. These two elements are part of the high resolution spectrometer rather than part of the transport system, and will be described in the section dealing with Experimental Equipment.

Experimental Equipment

The spectrometer will consist of a double focusing, uniform field magnet of 1.8 meter radius. It will bend the scattered particles through 90° and have unit magnification. The maximum aperture will accomodate a 200 mr acceptance in the bending plane (vertical) and a 40 mr acceptance in the scattering plane (horizontal). The system has a feature that allows the use of the full accelerator beam (with a 0.5% spectrum) in very high resolution electron scattering (approaching 1 part in 10^4) rather than discarding most of the intensity in energy defining slits. This technique, described below, was first used at lower resolutions in heavy ion scattering.[5]

To first order in the optics and neglecting recoil effects, one can obtain good resolution in reaction inelasticity while providing a wide incident energy spread on the target provided that the intrinsic resolution of the incident beam is good (that is, that the size the incident beam would have on target if it were monochromatic is sufficiently small) and provided that the dispersion of the incident beam is matched to the dispersion and magnification of the spectrometer (that is, dispersions equal for unity spectrometer magnification). In order to use this principle at high resolution, it is necessary to control certain aberrations, and for this purpose the magnet will be split-pole, composed of two 45° sections. Pole tip radii of curvature at entrance, between the sections, and at exit will be adjusted to make the three aberration coefficients (x/θ_0^2), $(x/\theta_0 x_0)$, and $(x/\theta_0 \gamma)$ simultaneously zero. The notation is that of K. Brown.[6] When this is done, neglecting recoil momenta and to second order in the aberrations, the full Beam C (0.5% energy spread) can be presented as a 4.6 x 1 cm^2 spot on target while obtaining resolution in reaction inelasticity of less than 2 x 10^{-4} with the full solid angle. With the full beam and at large scattering angles, recoil effects are a limiting factor at this resolution for target nuclei lighter than atomic number 60, but with the energy preselection capability of Beam C the technique will be useful for even the lightest nuclei. Ray tracing indicates that solid angles will actually be limited by higher order effects to values less than those quoted above, but some correction for these effects should be possible.

The purpose of the solenoid shown in Fig.4 is to rotate the plane of the dispersion produced in Beam C from the horizontal to the vertical before presenting the beam to the spectrometer target. The quadrupole Q7 in the figure is the fine control for matching beam and spectrometer dispersions. The spectrometer will bend downward, the magnet being supported over a semi-circular trench in which the focal plane array moves. Figure 5 illustrates the spectrometer. Figure 5 shows a section through the experimental area with the spectrometer at 90° to the beam. This arrangement is relatively simple mechanically and provides excellent detector shielding. For coincidence work, the area will also accommodate another spectrometer half the size of the large one.

References

1 J. Haimson, Nucl. Inst. Meth., 39, 13 (1966).

2 W.K.H. Panofsky, et al., Sci., 152,1353,(1966)

3 R. Helm, Proc. 1966, Lin. Acc. Conf., Los Alamos, 254, Oct. 1966.

4 J. Haimson, Proc. 1966 Lin. Acc. Conf., Los Alamos, 322, Oct. 1966.

5 B.L. Cohen, Rev. Sci. Inst., 30, 415, (1959).

6 K.L. Brown, Rev. Sci., Inst., 36, 271, (1965).

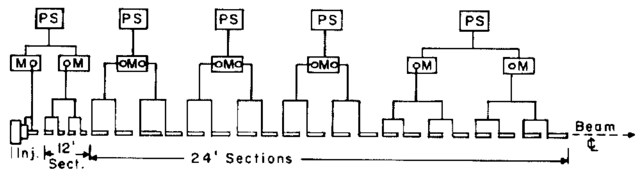

Fig. 1. Layout of beam centerline, modulators, and power supplies.

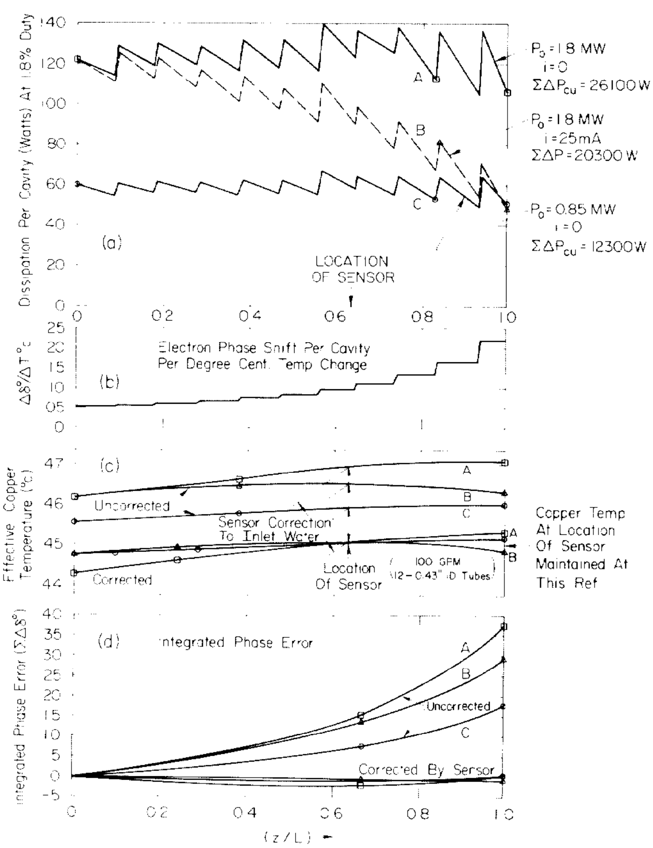

Fig. 2. Typical temperature phase characteristics for the 24' waveguide design.

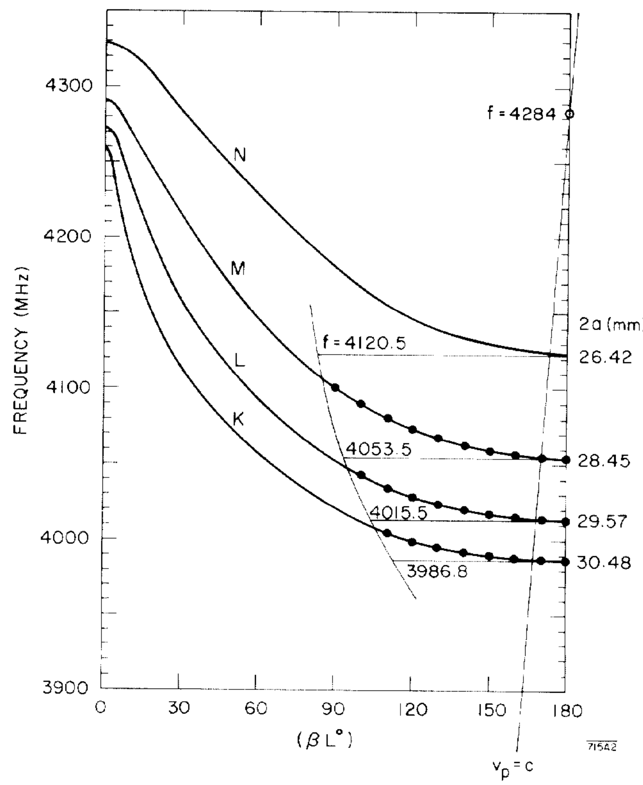

Fig. 3. TM_{11}-mode Brillouin diagrams indicating progressive stop-band separations.

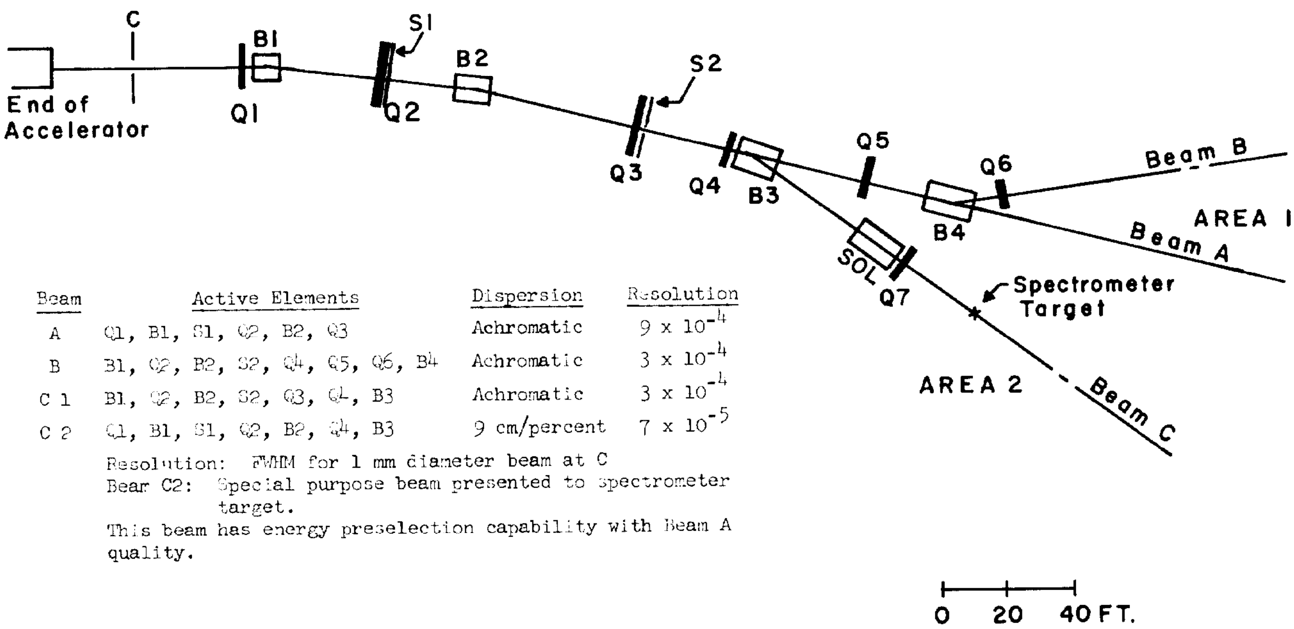

Beam	Active Elements	Dispersion	Resolution
A	Q1, B1, S1, Q2, B2, Q3	Achromatic	9×10^{-4}
B	B1, Q2, B2, S2, Q4, Q5, Q6, B4	Achromatic	3×10^{-4}
C 1	B1, Q2, B2, S2, Q3, Q4, B3	Achromatic	3×10^{-4}
C 2	Q1, B1, S1, Q2, B2, Q4, B3	9 cm/percent	7×10^{-5}

Resolution: FWHM for 1 mm diameter beam at C
Beam C2: Special purpose beam presented to spectrometer target.
This beam has energy preselection capability with Beam A quality.

Fig. 4. Beam transport system and beam characteristics.

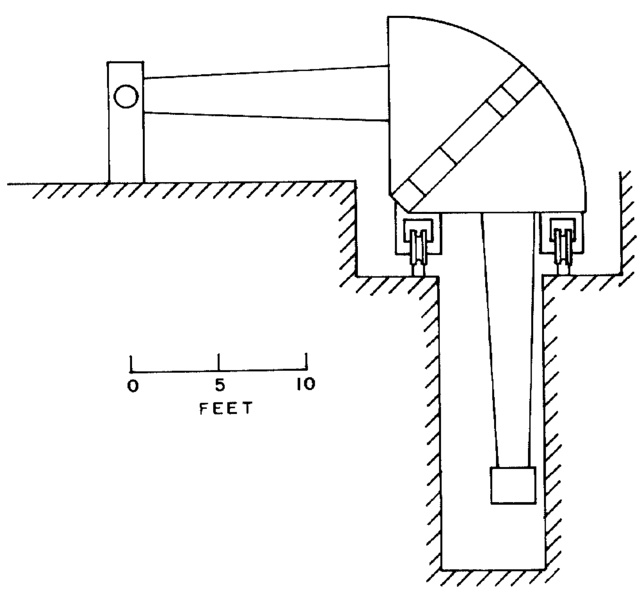

Fig. 5. Side view of target holder, vacuum chambers, and high-resolution split-pole spectrometer.